Toroidal Resonators for Electromagnetic Waves

FERDINAND CAP AND RUDOLF DEUTSCH

Abstract—**The solution of Maxwell's equations for toroidal systems has been reduced to the solution of the scalar Helmholtz equation. The eigenfunctions and the corresponding electromagnetic fields have been calculated analytically. The dispersion relation was formulated. Three different types of eigenmodes were obtained for each frequency. The structure of the electromagnetic field of the $m=0,1,2$, and 3 modes is analyzed.**

I. Introduction

TO OUR KNOWLEDGE no exact solution of the Helmholtz equation is known for toroidal coordinates [1]. On the other hand, such a solution is of interest not only for microwave engineering, but also for the heating of toroidal plasmas by electromagnetic waves. Using a special trick, we have been able to find a solution of the system of Maxwell equations not only for empty wave guides but also for resonators filled with an isotropic homogeneous plasma [2]. In the present paper we report on the vacuum solution, which resembles a little the solution by Brambilla and Finzi [3] but our solution is based on a different method and yields more eigenfunctions. Our solution admits an easy construction of the field for different modes and gives an interpretation of the dispersion relation.

During the elaboration of this paper, it was found that an exact unseparated solution of the same problem [4]. The solution presented here is of the separated form $f(\rho)\cdot g(\theta)$, whereas the exact solution is of the form $h(\rho,\theta)$. Using series expansions a comparison of the two solutions seems to be possible.

II. The Reduction of the Vector Helmholtz Equation to the Scalar Helmholtz Equation in Toroidal Coordinates

The coordinate system which we use is the usual ρ,θ,ϕ system [5] (see Fig. 1). We study the propagation of the electromagnetic waves on the basis of the vector Helmholtz equation

$$\operatorname{curl}\operatorname{curl}\vec{E}-\epsilon_0\mu_0\omega^2\vec{E}=0. \tag{1}$$

In order to find solutions of (1) which satisfy also Maxwell's set of equations we introduce the Hertz vector $\vec{P}$ in the usual form

$$\vec{E}=\epsilon_0\mu_0\omega^2\vec{P}+\operatorname{grad}\operatorname{div}\vec{P} \tag{2}$$

Manuscript received August 1, 1977; revised October 11, 1977.

The authors are with the Institute for Theoretical Physics, University of Innsbruck, Innrain 52, A-6020 Innsbruck, Austria.

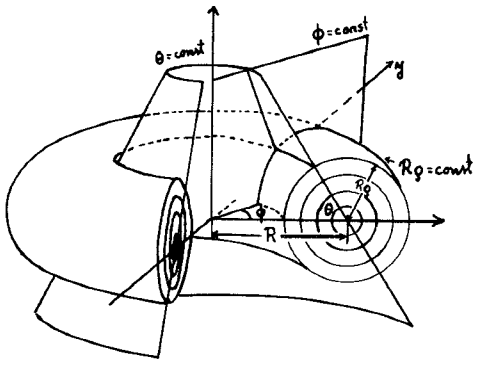

Fig. 1. The system of toroidal coordinates.

and

$$\vec{B}=i\omega\epsilon_0\mu_0\operatorname{curl}\vec{P}. \tag{3}$$

Exchanging $\vec{E}$ and $\vec{B}$ in (2) and (3), the Fitzgerald $\vec{F}$ vector could be used too. When $\vec{P}$ and $\vec{F}$ are known a general solution of Maxwell's equations can be written down. It is easy to show that (2) and (3) satisfy Maxwell's equations and also (1) if $\vec{P}$ satisfies

$$\operatorname{curl}\operatorname{curl}\vec{P}-\operatorname{grad}\operatorname{div}\vec{P}=\epsilon_0\mu_0\omega^2\vec{P}. \tag{4}$$

If we write (4) in toroidal coordinates a coupled system of three equations for the three components P_ρ, P_θ, and P_ϕ will be obtained. There is no possibility to obtain independent equations for each of these components as may be done in the case of Cartesian coordinates. But there is a way to construct the solution of equation (4) for the components P_ρ, P_θ, and P_ϕ using an idea, which somewhat resembles that used in [6] and [7]. In Cartesian coordinates (4) splits into the system of three equations:

$$\Delta P_j+\epsilon_0\mu_0\omega^2P_j=0 \tag{5}$$

for $j=x$, y, and z.

Equation (5) can be transformed to toroidal coordinates and the components P_j can be regarded as functions of ρ, θ, and ϕ. We then have to solve the scalar Helmholtz equation

$$\frac{\partial}{\partial\rho}\rho(1-\rho\cos\theta)\frac{\partial P_j}{\partial\rho}+\frac{\partial}{\partial\theta}\frac{(1-\rho\cos\theta)}{\rho}\frac{\partial P_j}{\partial\theta}+\frac{\rho}{1-\rho\cos\theta}\frac{\partial^2P_j}{\partial\phi^2}+k^2\rho(1-\rho\cos\theta)P_j=0 \tag{6}$$

0018-9480/78/0700-0478$00.75

where

$$k^2=\epsilon_0\mu_0\omega^2R^2=\left(\frac{\omega R}{c}\right)^2. \tag{7}$$

Here R is the major torus radius (Fig. 1).

Now using the coordinate transformation for the covariant components of a vector we can express P_ρ, P_θ, and P_ϕ through P_x, P_y, and P_z in the following form:

$$\begin{aligned}P_\rho(\rho,\theta,\phi)&=-P_x(\rho,\theta,\phi)\cos\theta\cos\phi\\&\quad-P_y(\rho,\theta,\phi)\cos\theta\sin\phi+P_z(\rho,\theta,\phi)\sin\theta\\P_\theta(\rho,\theta,\phi)&=P_x(\rho,\theta,\phi)\sin\theta\cos\phi\\&\quad+P_y(\rho,\theta,\phi)\sin\theta\sin\phi+P_z(\rho,\theta,\phi)\cos\theta\\P_\phi(\rho,\theta,\phi)&=-P_x(\rho,\theta,\phi)\sin\phi+P_y(\rho,\theta,\phi)\cos\phi.\end{aligned} \tag{8}$$

So we were able to "scalarize" the vector (1), i.e., to reduce it to a single scalar (6).

III. The Solution of the Scalar Helmholtz Equation in Toroidal Coordinates

The scalar Helmholtz (6) is however also not separable in toroidal coordinates [8], but it can be solved. In order to do this we make the substitution

$$P_j(\rho,\theta,\phi)=\frac{\psi_m(\rho,\theta)e^{im\phi}}{\sqrt{1-\rho\cos\theta}}. \tag{9}$$

Inserting into (6) we obtain

$$\frac{\partial^2\psi_m}{\partial\rho^2}+\frac{1}{\rho}\frac{\partial\psi_m}{\partial\rho}+\frac{1}{\rho^2}\frac{\partial^2\psi_m}{\partial\theta^2}+k^2\psi_m=\frac{m^2-1/4}{(1-\rho\cos\theta)^2}\psi_m. \tag{10}$$

The expression from the right-hand side vanishes if $m=1/2$. We gave this exact solution in [5] and [11]. It has, however, a period of 4π and therefore it does not correspond to an empty torus. We will analyze the physical consequences of this solution in another paper [11].

If $m\neq 1/2$ the right-hand side of (10) does not vanish. Since separation between ρ and θ is impossible we expand the right-hand side term

$$(1-\rho\cos\theta)^2=\sum_{n=0}^{\infty}(n+1)\rho^n\cos^n\theta. \tag{11}$$

This series converges for $\rho<1$. For experimental toroidal systems the maximal value of the inverse aspect ratio ρ is about 0.3. In this case the error is about 10^{-4} if we take into account all terms including the term $\sim\rho^{-4}$. Inserting (11) into (10) we obtain

$$\frac{1}{\rho}\frac{\partial}{\partial\rho}\left(\rho\frac{\partial\psi_m}{\partial\rho}\right)+\frac{1}{\rho^2}\frac{\partial^2\psi_m}{\partial\theta^2}+\kappa^2\psi_m=\mu^2\psi_m\sum_{n=1}^{\infty}(n+1)\rho^n\cos^n\theta \tag{12}$$

where

$$\kappa^2=k^2-m^2+\frac{1}{4} \tag{13}$$

and

$$\mu^2=m^2-\frac{1}{4}. \tag{14}$$

If we limit our calculations to the waves, whose longitudinal wavelength ($2\pi R/m$) in the torus exceeds the dimension of the transversal circular sections of one branch of the torus ($2R\rho_0$), or if condition

$$m\rho_0<\pi \tag{15}$$

(ρ_0 is the inverse aspect ratio of the torus) is satisfied, the solution of (12) can be written in the form

$$\psi_m=\psi_{m,0}+\psi_{m,1}+\psi_{m,2}+\psi_{m,3}+\cdots+\psi_{m,n}+ \tag{16}$$

where the functions $\psi_{m,n}$ are solutions of the equations

$$\frac{1}{\rho}\frac{\partial}{\partial\rho}\left(\rho\frac{\partial\psi_{m,0}}{\partial\rho}\right)+\frac{1}{\rho^2}\frac{\partial^2\psi_{m,0}}{\partial\theta^2}+\kappa^2\psi_{m,0}=0 \tag{17}$$

$$\frac{1}{\rho}\frac{\partial}{\partial\rho}\left(\rho\frac{\partial\psi_{m,1}}{\partial\rho}\right)+\frac{1}{\rho^2}\frac{\partial^2\psi_{m,1}}{\partial\theta^2}+\kappa^2\psi_{m,1}=2\mu^2\rho\cos\theta\psi_{m,0} \tag{18}$$

$$\frac{1}{\rho}\frac{\partial}{\partial\rho}\left(\rho\frac{\partial\psi_{m,2}}{\partial\rho}\right)+\frac{1}{\rho^2}\frac{\partial^2\psi_{m,2}}{\partial\theta^2}+\kappa^2\psi_{m,2}=2\mu^2\rho\cos\theta\psi_{m,1}+3\mu^2\rho^2\cos^2\theta\psi_{m,0} \tag{19}$$

$$\frac{1}{\rho}\frac{\partial}{\partial\rho}\left(\rho\frac{\partial\psi_{m,3}}{\partial\rho}\right)+\frac{1}{\rho^2}\frac{\partial^2\psi_{m,3}}{\partial\theta^2}+\kappa^2\psi_{m,3}=2\mu^2\rho\cos\theta\psi_{m,2}+3\mu^2\rho^2\cos^2\theta\psi_{m,1}+4\mu^2\rho^3\cos^3\theta\psi_{m,2}. \tag{20}$$

The solution of (17) which is everywhere finite is given by the Bessel functions

$$\psi_{m,0}=AJ_\nu(\kappa\rho)\cos\nu\theta. \tag{21}$$

If we insert this expression in the right-hand side of (18) and solve the equation we get for the first correction to (21):

$$\psi_{m,1}=\frac{A\mu^2}{4\kappa}\left[J_{\nu+1}(\kappa\rho)\cos(\nu-1)\theta-J_{\nu-1}(\kappa\rho)\cos(\nu+1)\theta\right]\rho^2. \tag{22}$$

Inserting (21) and (22) in (19) and solving the equation we get the second approximation. Continuing this method we can calculate the corrections to an arbitrary order of accuracy. Our calculations will be restricted to the lowest ν modes. In this case we get for the sum (16), for various

values of ν in the approximation up to the terms with $\cos 4\theta$, the following functions ($\kappa\rho = z$). For $\nu = 0$, 1, 2, 3, and 4 we get

$$\begin{aligned}
\psi_{m,\nu=0} = A\Bigg\{ & J_0(z) + \frac{\gamma_1^2}{64}J_2(z)z^4 - \frac{\gamma_1^2}{96}J_3(z)z^3 \\
& + \frac{\gamma_2}{12}[J_1(z)z - J_2(z)]z^2 + \frac{\gamma_1^4}{7225344}J_8(z)z^8 \\
& - \frac{\gamma_1^4}{150528}J_6(z)z^8 + \frac{\gamma_1^4}{18432}J_4(z)z^8 \\
& + \left(\frac{\gamma_1^4}{387072} + \frac{\gamma_1^2\gamma_2}{115200}\right)J_7(z)z^7 \\
& - \left(\frac{5\gamma_1^4}{55296} + \frac{7\gamma_1^2\gamma_2}{23040}\right)J_5(z)z^7 + \frac{21\gamma_1^2\gamma_2}{12800}J_3(z)z^7 \\
& + \left(\frac{\gamma_1^2\gamma_2}{11520} + \frac{3\gamma_1\gamma_3}{25600} + \frac{\gamma_2^2}{19200}\right)J_6(z)z^6 \\
& - \left(\frac{\gamma_1^2\gamma_2}{480} + \frac{9\gamma_1\gamma_3}{3200} + \frac{\gamma_2^2}{800}\right)J_4(z)z^6 \\
& + \left(\frac{9\gamma_1\gamma_3}{1024} + \frac{\gamma_2^2}{256}\right)J_2(z)z^6 \\
& + \left(\frac{\gamma_1\gamma_3}{2560} + \frac{\gamma_2^2}{3840} + \frac{\gamma_4}{960}\right)J_5(z)z^5 \\
& - \left(\frac{3\gamma_1\gamma_3}{512} + \frac{\gamma_2^2}{256} + \frac{\gamma_4}{64}\right)J_3(z)z^5 + \frac{\gamma_4}{48}J_1(z)z^5 \\
& + \Bigg[\frac{\gamma_1}{4}J_1(z) - \frac{\gamma_1^3}{1536}(4J_4(z) - 3zJ_3(z))z^3 \\
& - \frac{\gamma_1\gamma_2}{96}(4J_3(z) - 3zJ_2(x))z^2 \\
& - \frac{\gamma_3}{32}(4J_2(z) - 3zJ_1(z))z\Bigg]z^2\cos\theta \\
& + \Bigg[\frac{\gamma_1^2}{64}zJ_2(z) + \frac{\gamma_2}{12}J_1(z) - \frac{\gamma_1^4}{143360}z^5J_6(z) \\
& + \frac{\gamma_1^4}{13440}z^5J_4(z) - \left(\frac{\gamma_1^4}{10752} + \frac{\gamma_1^2\gamma_2}{3072}\right)z^4J_5(z) \\
& + \frac{7\gamma_1^2\gamma_2}{3072}z^4J_3(z) - \left(\frac{5\gamma_1^2\gamma_2}{2304} + \frac{\gamma_1\gamma_3}{320} + \frac{\gamma_2^2}{720}\right)z^3J_4(z) \\
& + \left(\frac{\gamma_1\gamma_3}{80} + \frac{\gamma_2^2}{180}\right)z^3J_2(z) \\
& - \left(\frac{\gamma_1\gamma_3}{160} + \frac{\gamma_2^2}{240} + \frac{3\gamma_4}{160}\right)z^2J_3(z) \\
& + \frac{\gamma_4}{32}z^2J_1(z)\Bigg]z^3\cos 2\theta \\
& + \left[\frac{\gamma_1^3}{1536}z^2J_3(z) + \frac{\gamma_1\gamma_2}{96}zJ_2(z) + \frac{\gamma_3}{32}J_1(z)\right]z^4\cos 3\theta \\
& + \Bigg[\frac{\gamma_1^4}{49152}z^3J_4(z) + \frac{\gamma_1^2\gamma_2}{1536}z^2J_3(z) \\
& + \left(\frac{\gamma_1\gamma_3}{256} + \frac{\gamma_2^2}{576}\right)zJ_2(z) + \frac{\gamma_4}{80}J_1(z)\Bigg]z^5\cos 4\theta\Bigg\} \qquad (23)
\end{aligned}$$

and omitting the argument z of the Bessel functions

$$\begin{aligned}
\psi_{m,\nu=1} = B\Bigg\{ & \frac{\gamma_1}{8}z^2J_2 - \frac{\gamma_1^3}{30720}z^6J_6 + \frac{\gamma_1^3}{1280}z^6J_4 \\
& - \frac{\gamma_1^3}{6144}z^6J_2 - \frac{\gamma_1\gamma_2}{1152}z^5J_5 + \frac{5\gamma_1\gamma_2}{384}z^5J_3 \\
& - \frac{\gamma_1\gamma_2}{576}z^5J_1 - \frac{\gamma_3}{192}z^4J_4 + \frac{\gamma_3}{24}z^4J_2 \\
& + \left[J_1 + \frac{\gamma_1^2}{384}z^4(7J_3 - 2J_1) + \frac{\gamma_2}{8}z^3J_2\right]\cos\theta \\
& + \Bigg[-\frac{\gamma_1}{8}z^2J_0 + \frac{\gamma_1^3}{1152}z^6J_4 + \frac{\gamma_1^3}{2304}z^6J_2 \\
& + \frac{\gamma_1\gamma_2}{3840}z^5J_7 + \frac{\gamma_1\gamma_2}{768}z^5J_5 + \frac{23\gamma_1\gamma_2}{1280}z^5J_3 \\
& - \frac{\gamma_1\gamma_2}{256}z^5J_1 + \frac{\gamma_3}{16}z^4J_2\Bigg]\cos 2\theta \\
& + \left[-\frac{\gamma_1^2}{128}z^4J_1 + \frac{\gamma_2}{240}z^3(J_6 + 6J_4 + 15J_2)\right]\cos 3\theta \\
& + \Bigg[-\frac{\gamma_1^3}{3072}z^6J_2 + \frac{\gamma_1\gamma_2}{17920}z^5J_9 + \frac{\gamma_1\gamma_2}{1536}z^5J_7 \\
& + \frac{13\gamma_1\gamma_2}{5376}z^5J_5 + \frac{\gamma_1\gamma_2}{256}z^5J_3 \\
& + \frac{\gamma_1\gamma_2}{320}z^5J_1 - \frac{\gamma_3}{64}z^4J_0\Bigg]\cos 4\theta\Bigg\}. \qquad (24)
\end{aligned}$$

$$\begin{aligned}
\psi_{m,\nu=2} = C\Bigg\{ & \frac{\gamma_1^2}{128}z^4J_4 + \frac{\gamma_2}{24}z^3J_3 + \frac{\gamma_1}{8}z^2J_3\cos\theta \\
& + \Bigg[J_2 + \frac{\gamma_1^2}{1920}z^4(J_6 + 16J_4 - 15J_2) \\
& + \frac{\gamma_2}{96}z^3(J_5 + 9J_3)\Bigg]\cos 2\theta
\end{aligned}$$

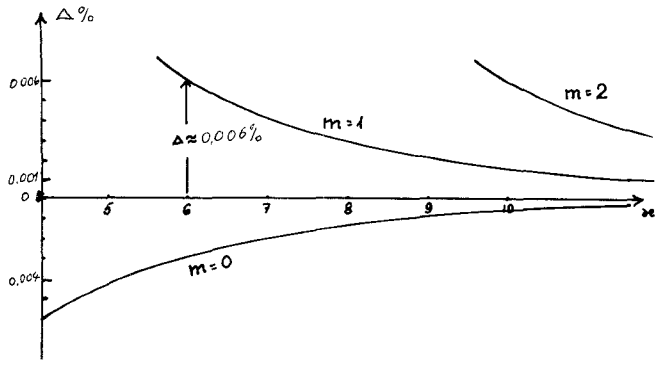

Fig. 2. The maximum error in determining Δ for different κ and m.

$$-\frac{\gamma_1}{8}z^2J_1\cos 3\theta+\left[\frac{\gamma_1^2}{128}z^4J_0-\frac{\gamma_2}{24}z^3J_1\right]\cos 4\theta\Bigg\} \quad (25)$$

$$\psi_{m,\nu=3}=\boldsymbol{D}\left\{\frac{\gamma_1}{8}z^2J_4\cos 2\theta+J_3\cos 3\theta-\frac{\gamma_1}{8}z^2J_2\cos 4\theta\right\} \quad (26)$$

$$\psi_{m,\nu=4}=\boldsymbol{E}J_4\cos 4\theta. \quad (27)$$

Here we used the notations $z=\kappa\rho$ and $\gamma_j=(j+1)\mu^2/\kappa^{j+2}$. All Bessel functions J_i are functions of $\kappa\rho$. The solution ψ_m of (10) is a superposition of the functions (23)–(27). The constants $\boldsymbol{B}$, $\boldsymbol{C}$, $\boldsymbol{D}$, and $\boldsymbol{E}$ are determined by the boundary conditions. For conducting torus walls $\boldsymbol{B}_\rho=0$ must be satisfied at the boundary $\rho=\rho_0$. This can be realized in agreement with (3), (8), and (9) if ψ_m itself vanishes at the boundary. Condition

$$\psi_m=\psi_{m,\nu=0}+\psi_{m,\nu=1}+\psi_{m,\nu=2}+\psi_{m,\nu=3}+\psi_{m,\nu=4}=0 \quad (28)$$

leads to five conditions which determine $\boldsymbol{B}$, $\boldsymbol{C}$, $\boldsymbol{D}$, $\boldsymbol{E}$, and the product $\kappa\rho_0$. A very good convergence of the series

$$\psi_m=\psi_{m,\nu=0}+\psi_{m,\nu=1}+\psi_{m,\nu=2}+\psi_{m,\nu=3}+\psi_{m,\nu=4}+\cdots \quad (29)$$

was found. In Fig. 2 we have plotted the deviation of the product $\kappa\rho_0$ from the value 2.4048255577 (corresponding to the first root of the Bessel function J_0) for different $\boldsymbol{m}$ if we use the method described above. The relative deviation

$$\Delta=\frac{\kappa\rho_0-2.4048255577}{\kappa\rho_0}$$

is expressed as a function of κ in the interval of practical interest. It can be seen that it is generally less than 10^{-3}. This means that the approximation

$$\psi_m=AJ_0(\kappa\rho) \quad (30)$$

leads to a good description of the structure of the electromagnetic field and that

$$\kappa\rho_0=2.4048 \quad (31)$$

can be used to determine the dependence of the parameter κ from the inverse aspect ratio ρ_0.

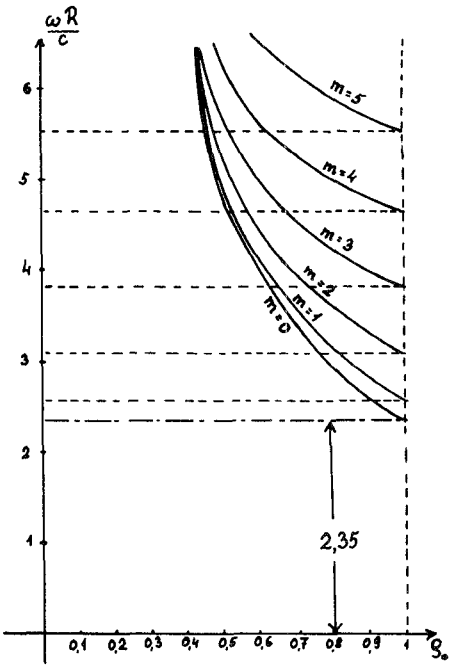

Fig. 3. The dependence of the eigenfrequency on the inverse aspect ratio of the torus.

IV. The Dispersion Relation

Now using (7), (13), and (31) the dispersion relation results

$$\omega^2=\left(\frac{5.7832}{\rho_0^2}+m^2-\frac{1}{4}\right)\frac{c^2}{R^2}. \quad (32)$$

If we now take into account that

$$\rho_0<1 \quad (33)$$

then the eigenfrequencies are always greater than

$$\omega_{min}^{(m)}=\frac{c}{R}\sqrt{m^2+5.5332}. \quad (34)$$

The dependence of the eigenfrequencies on the inverse aspect ratio ρ_0 for different mode numbers $\boldsymbol{m}$ is given in Fig. 3. The distance between two different eigenfrequencies is of the same order as the minimum frequency.

In the whole domain of applicability of our method the dispersion relation (32) can be approximated by the series

$$\frac{\omega R}{c}=\frac{2.4048}{\rho_0}+\frac{\rho_0}{4.8096}\left(m^2-\frac{1}{4}\right)-\frac{\rho_0^3}{111.6}\left(m^2-\frac{1}{4}\right)^2+\cdots. \quad (35)$$

V. The Structure of the Electromagnetic Field in the Torus

Now we shall use the approximation (30) to construct the field components of the stationary electromagnetic wave in the torus. These fields all correspond to the lowest θ mode.

Inserting (30) into (9) we get two possibilities to choose

the Cartesian components of the Hertz vector

$$P_j(\rho,\theta,\phi)=\frac{J_0(\kappa\rho)\cos m\phi}{\sqrt{1-\rho\cos\theta}}e^{i\omega t} \tag{36}$$

and/or

$$P_j(\rho,\theta,\phi)=\frac{J_0(\kappa\rho)\sin m\phi}{\sqrt{1-\rho\cos\theta}}e^{i\omega t}. \tag{37}$$

We shall use these functions to construct the toroidal components of the Hertz vector using formulas (8).

It is possible to define some normal modes and to get all stationary waves with the same value of m as a superposition of these modes.

A. Toroidal Modes of the First Type

If

$$P_x=P_y=0 \text{ and } P_z=\frac{J_0(\kappa\rho)\cos m\phi}{\sqrt{1-\rho\cos\theta}}e^{i\omega t} \tag{38}$$

the toroidal components of the Hertz vector are

$$\begin{aligned} P_\rho &= \frac{J_0(\kappa\rho)\sin\theta\cos m\phi}{\sqrt{1-\rho\cos\theta}}e^{i\omega t} \\ P_\theta &= \frac{J_0(\kappa\rho)\cos\theta\cos m\phi}{\sqrt{1-\rho\cos\theta}}e^{i\omega t} \\ P_\phi &= 0. \end{aligned} \tag{39}$$

Using (2) we obtain for the components of the electric field

$$E_\rho=\left[\left(m^2-\frac{1}{4}\right)\frac{J_0(\kappa\rho)}{\sqrt{1-\rho\cos\theta}}+\frac{\kappa}{2\rho}\frac{2-3\rho\cos\theta}{\sqrt{(1-\rho\cos\theta)^3}}J_1(\kappa\rho)\right] \cdot\sin\theta\cos m\phi e^{i\omega t} \tag{40}$$

$$E_\theta=\left[\frac{\kappa^2+m^2-\frac{1}{4}}{\sqrt{1-\rho\cos\theta}}J_0(\kappa\rho)-\frac{\kappa J_1(\kappa\rho)}{\rho\sqrt{1-\rho\cos\theta}}\right] \cdot\cos\theta\cos m\phi e^{i\omega t}+\frac{\kappa J_1(\kappa\rho)\sin^2\theta\cos m\phi}{2\sqrt{(1-\rho\cos\theta)^3}}e^{i\omega t} \tag{41}$$

$$E_\phi=\frac{m\kappa J_1(\kappa\rho)\sin\theta\sin m\phi}{\sqrt{(1-\rho\cos\theta)^3}}e^{i\omega t}. \tag{42}$$

For the components of the magnetic field results from (3) and (39)

$$B_\rho=i\omega\epsilon\mu\frac{mJ_0(\kappa\rho)\cos\theta\sin m\phi}{\sqrt{(1-\rho\cos\theta)^3}}e^{i\omega t} \tag{43}$$

$$B_\theta=-i\omega\epsilon\mu\frac{mJ_0(\kappa\rho)\sin\theta\sin m\phi}{\sqrt{(1-\rho\cos\theta)^3}}e^{i\omega t} \tag{44}$$

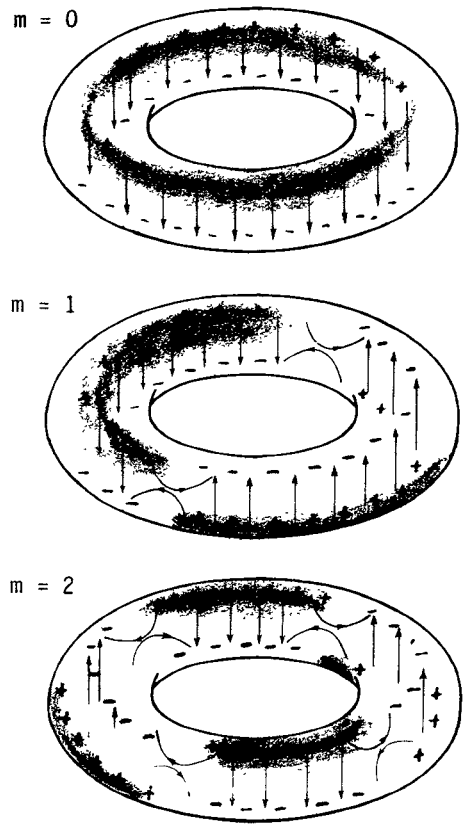

Fig. 4. Toroidal modes of first type. Electric field and surface charge distribution.

$$B_\phi=i\omega\epsilon\mu\frac{J_0(\kappa\rho)-2\kappa(1-\rho\cos\theta)J_1(\kappa\rho)\cos\theta}{2\sqrt{(1-\rho\cos\theta)^3}}\cos m\phi e^{i\omega t}. \tag{45}$$

For the charge surface density the following relation results:

$$\sigma\sim\frac{2-3\rho_0\cos\theta}{\sqrt{(1-\rho_0\cos\theta)^3}}\sin\theta\cos m\phi e^{i\omega t}. \tag{46}$$

The distribution of the surface charge and the electric field lines in the interior of the torus are represented for $m=0$, $m=1$, and $m=2$ in Fig. 4. As can be seen there appear dipolar, quadrupolar, octupolar, etc. oscillations of the electric charges in the inner side of the toroidal surface. The changes of the electric field and the surface currents create a magnetic field with oscillations shifted by 90° in phase and described by (43)–(45). The equations of the magnetic field lines can be integrated analytically. We obtain

$$z=\rho\sin\theta=k_1 \tag{47}$$

and

$$\frac{J_0(\kappa\rho)}{\sqrt{1-\rho\cos\theta}}\cos m\phi=k_2. \tag{48}$$

They are represented in Fig. 5 for $m=0$, $m=1$, and $m=2$.

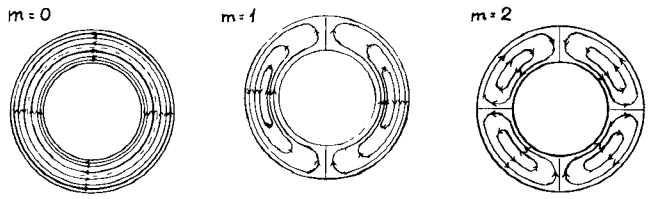

Fig. 5. Toroidal modes of first type. Magnetic field lines.

Remark: If we use for P_z in (38) the component (37) instead of (36) we get similar fields, which are, however, rotated by $\pi/2m$ around the z axis.

B. Toroidal Modes of the Second Type

For

$$P_x = \frac{J_0(\kappa\rho)\cos m\phi}{\sqrt{1-\rho\cos\theta}} e^{i\omega t}, \qquad P_y = P_z = 0 \tag{49}$$

another type of toroidal modes results. These modes are described by

$$P_\rho = -\frac{J_0(\kappa\rho)\cos\theta}{2\sqrt{1-\rho\cos\theta}}\left[\cos(m+1)\phi+\cos(m-1)\phi\right]e^{i\omega t} \tag{50}$$

$$P_\theta = \frac{J_0(\kappa\rho)\sin\theta}{2\sqrt{1-\rho\cos\theta}}\left[\cos(m+1)\phi+\cos(m-1)\phi\right]e^{i\omega t} \tag{51}$$

$$P_\phi = -\frac{J_0(\kappa\rho)}{2\sqrt{1-\rho\cos\theta}}\left[\sin(m+1)\phi-\sin(m-1)\phi\right]e^{i\omega t}. \tag{52}$$

The components of the electric and magnetic fields are

$$E_\rho = \left\{-\frac{J_0(\kappa\rho)\cos\theta}{2\sqrt{1-\rho\cos\theta}}\left[\frac{3}{4(1-\rho\cos\theta)^2}+m^2-\frac{1}{4}\right] + \frac{\kappa}{2\rho}\frac{J_1(\kappa\rho)\cos\theta}{\sqrt{(1-\rho\cos\theta)^3}}\cdot\left[(1+3\cos^2\theta)\rho-2\cos\theta\right]\right\} \cdot\left[\cos(m+1)\phi+\cos(m-1)\phi\right]e^{i\omega t} + m\left[\frac{\kappa}{2}\frac{J_1(\kappa\rho)}{\sqrt{(1-\rho\cos\theta)^3}}-\frac{3J_0(\kappa\rho)\cos\theta}{4\sqrt{(1-\rho\cos\theta)^5}}\right] \cdot\left[\cos(m+1)\phi-\cos(m-1)\phi\right]e^{i\omega t} \tag{53}$$

$$E_\theta = \left\{\frac{J_0(\kappa\rho)\sin\theta}{2\sqrt{1-\rho\cos\theta}}\left[\kappa^2+m^2-\frac{1}{4}+\frac{3}{4(1-\rho\cos\theta)^2}\right] - \frac{\kappa J_1(\kappa\rho)\sin\theta}{4\rho\sqrt{(1-\rho\cos\theta)^3}}\cdot(2-\rho\cos\theta)\right\} \cdot\left[\cos(m+1)\phi+\cos(m-1)\phi\right]e^{i\omega t} + \frac{3mJ_0(\kappa\rho)\sin\theta}{4\sqrt{(1-\rho\cos\theta)^5}}\cdot\left[\cos(m+1)\phi-\cos(m-1)\phi\right]e^{i\omega t} \tag{54}$$

$$E_\phi = \left\{\frac{J_0(\kappa\rho)}{4\sqrt{(1-\rho\cos\theta)^5}}\left[1+2m^2-2(1-\rho\cos\theta)^2 \cdot\left(\kappa^2+m^2-\frac{1}{4}\right)\right]-\frac{\kappa J_1(\kappa\rho)\cos\theta}{2\sqrt{(1-\rho\cos\theta)^3}}\right\} \cdot\left[\sin(m+1)\phi-\sin(m-1)\phi\right]e^{i\omega t} + m\left\{\frac{3J_0(\kappa\rho)}{4\sqrt{(1-\rho\cos\theta)^5}}-\frac{\kappa J_1(\kappa\rho)\cos\theta}{2\sqrt{(1-\rho\cos\theta)^3}}\right\} \cdot\left[\sin(m+1)\phi+\sin(m-1)\phi\right]e^{i\omega t} \tag{55}$$

$$B_\rho = i\frac{\omega\epsilon\mu J_0(\kappa\rho)\sin\theta}{2\sqrt{(1-\rho\cos\alpha)^3}}\left[m(\sin(m+1)\phi+\sin(m-1)\phi) + \frac{1}{2}(\sin(m+1)\phi-\sin(m-1)\phi)\right]e^{i\omega t} \tag{56}$$

$$B_\theta = i\frac{\omega\epsilon\mu}{2}\left[\frac{J_0(\kappa\rho)\cos\theta}{2\sqrt{(1-\rho\cos\theta)^3}}-\frac{\kappa J_1(\kappa\rho)}{\sqrt{1-\rho\cos\theta}}\right] \cdot\left[\sin(m+1)\phi-\sin(m-1)\phi\right]e^{i\omega t} + i\frac{\omega\epsilon\mu m J_0(\kappa\rho)\cos\theta}{2\sqrt{(1-\rho\cos\theta)^3}}\left[\sin(m+1)\phi+\sin(m-1)\phi\right]e^{i\omega t} \tag{57}$$

$$B_\phi = -i\frac{\omega\epsilon\mu\kappa J_1(\kappa\rho)\sin\theta}{2\sqrt{1-\rho\cos\theta}}\left[\cos(m+1)\phi+\cos(m-1)\phi\right]e^{i\omega t}. \tag{58}$$

The charge density on the surface of the torus is proportional to

$$\sigma \sim \frac{(1+3\cos^2\theta)\rho_0-2\cos\theta}{2\rho_0\sqrt{(1-\rho_0\cos\theta)^3}}\left[\cos(m+1)\phi-\cos(m-1)\phi\right]e^{i\omega t} + \frac{m}{\sqrt{(1-\rho_0\cos\theta)^3}}\left[\cos(m+1)\phi-\cos(m-1)\phi\right]e^{i\omega t}. \tag{59}$$

The electric field and the surface charge distribution are represented in Figs. 6–9. The magnetic field lines are given by

$$x = (1-\rho\cos\theta)\cos\phi = k_1 \tag{60}$$

and

$$J_0(\kappa\rho)\cos m\phi\sqrt{\cos\phi} = k_2. \tag{61}$$

They form vortices in parallel planes which are situated perpendicular to the plane of the torus. The electric field has a three-dimensional structure. We tried to show this representing the field lines for different sections of the torus. For $m=0$ a simple dipolar polarization appears. For high m values the field structure will be more complicated.

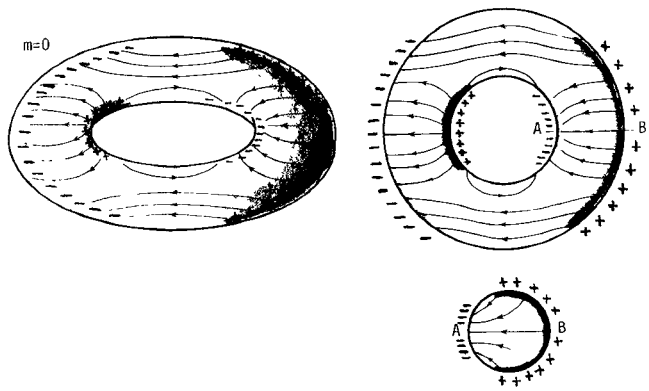

Fig. 6. Toroidal mode of second type. Electric field and surface charge distribution.

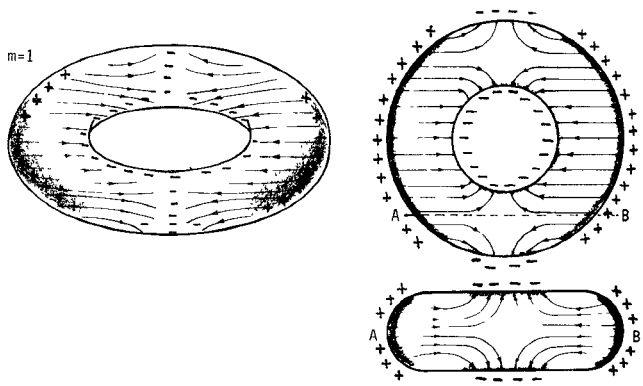

Fig. 7. Toroidal mode of second type. Electric field and surface charge distribution.

There appear some regions with greater charge concentrations which are shown in the figures.

C. Toroidal Modes of the Third Type

If

$$P_x = \frac{J_0(\kappa\rho)\sin m\phi}{\sqrt{1-\rho\cos\theta}}\, e^{i\omega t}, \qquad P_y = P_z = 0 \tag{62}$$

the toroidal components of the Hertz vector will be

$$P_\rho = -\frac{J_0(\kappa\rho)\cos\theta}{2\sqrt{1-\rho\cos\theta}}\left[\sin(m+1)\phi+\sin(m-1)\phi\right]e^{i\omega t} \tag{63}$$

$$P_\theta = \frac{J_0(\kappa\rho)\sin\theta}{2\sqrt{1-\rho\cos\theta}}\left[\sin(m+1)\phi+\sin(m-1)\phi\right]e^{i\omega t} \tag{64}$$

$$P_\phi = \frac{J_0(\kappa\rho)}{2\sqrt{1-\rho\cos\theta}}\left[\cos(m+1)\phi-\cos(m-1)\phi\right]e^{i\omega t}. \tag{65}$$

The components of the electric and magnetic fields are

$$E_\rho = \left\{\frac{\kappa J_1(\kappa\rho)}{4\rho\sqrt{(1-\rho\cos\theta)^3}}\left[(1+3\cos^2\theta)\rho-2\cos\theta\right]\right.$$

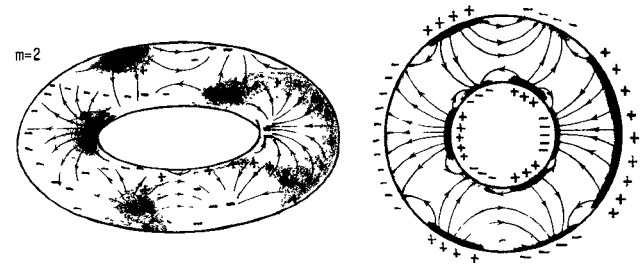

Fig. 8. Toroidal mode of second type. Electric field and surface charge distribution.

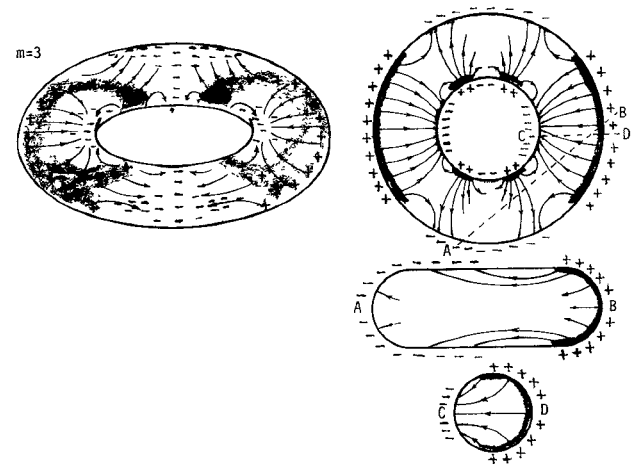

Fig. 9. Toroidal mode of second type. Electric field and surface charge distribution.

$$\left.-\frac{J_0(\kappa\rho)\cos\theta}{2\sqrt{(1-\rho\cos\theta)^5}}\cdot\left[\frac{3}{4}+\left(m^2-\frac{1}{4}\right)(1-\rho\cos\theta)^2\right]\right\}$$
$$\cdot\left[\sin(m+1)\phi+\sin(m-1)\phi\right]e^{i\omega t}$$
$$+m\left[\frac{\kappa J_1(\kappa\rho)}{2\sqrt{(1-\rho\cos\theta)^3}}-\frac{3J_0(\kappa\rho)\cos\theta}{4\sqrt{(1-\rho\cos\theta)^5}}\right]$$
$$\cdot\left[\sin(m+1)\phi-\sin(m-1)\phi\right]e^{i\omega t} \tag{66}$$

$$E_\theta = \left\{\frac{J_0(\kappa\rho)\sin\theta}{2\sqrt{(1-\rho\cos\theta)^5}}\right.$$
$$\cdot\left[\left(\kappa^2+m^2-\frac{1}{4}\right)(1-\rho\cos\theta)^2+\frac{3}{4}\right]$$
$$\left.-\frac{\kappa J_1(\kappa\rho)\sin\theta}{4\rho\sqrt{(1-\rho\cos\theta)^3}}(2-\rho\cos\theta)\right\}$$
$$\cdot\left[\sin(m+1)\phi+\sin(m-1)\phi\right]e^{i\omega t}$$
$$+\frac{3mJ_0(\kappa\rho)\sin\theta}{4\sqrt{(1-\rho\cos\theta)^5}}\left[\sin(m+1)\phi-\sin(m-1)\phi\right]e^{i\omega t}. \tag{67}$$

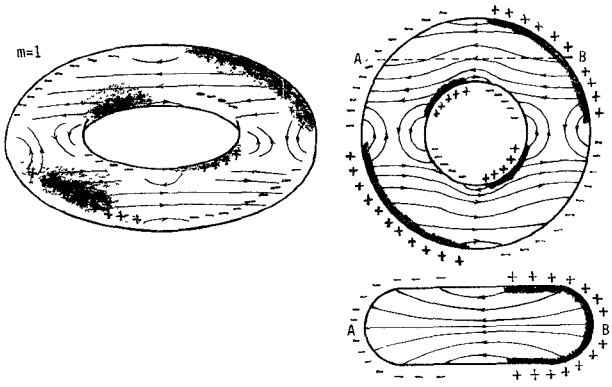

Fig. 10. Toroidal mode of third type. Electric field and surface charge distribution.

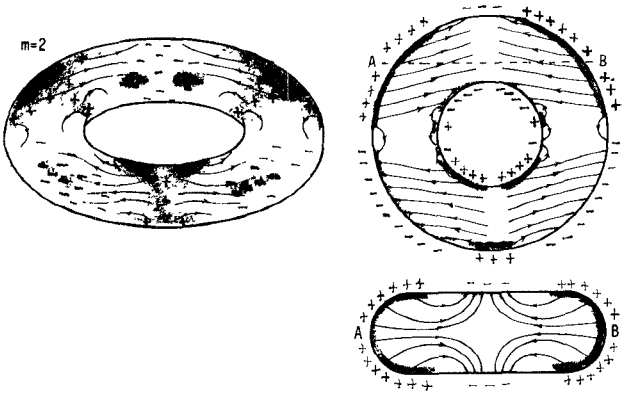

Fig. 11. Toroidal mode of third type. Electric field and surface charge distribution.

$$E_\phi = \left\{ \frac{J_0(\kappa\rho)}{2\sqrt{1-\rho\cos\theta}} \left[\kappa^2 + m^2 - \frac{1}{4} - \frac{1+2m^2}{2(1-\rho\cos\theta)^2} \right] + \frac{\kappa J_1(\kappa\rho)\cos\theta}{2\sqrt{(1-\rho\cos\theta)^3}} \right\} \cdot \left[\cos(m+1)\phi - \cos(m-1)\phi \right] e^{i\omega t}$$

$$+ m \left[\frac{\kappa J_1(\kappa\rho)\cos\theta}{2\sqrt{(1-\rho\cos\theta)^3}} - \frac{3J_0(\kappa\rho)}{4\sqrt{(1-\rho\cos\theta)^5}} \right] \cdot \left[\cos(m+1)\phi + \cos(m-1)\phi \right] e^{i\omega t}. \quad (68)$$

$$B_\rho = -i\omega\epsilon\mu \frac{J_0(\kappa\rho)\sin\theta}{2\sqrt{(1-\rho\cos\theta)^3}} \left[m(\cos(m+1)\phi + \cos(m-1)\phi) + \frac{1}{2}(\cos(m+1)\phi - \cos(m-1)\phi) \right] e^{i\omega t}. \quad (69)$$

$$B_\theta = -i\omega\epsilon\mu \left\{ \left[\frac{J_0(\kappa\rho)\cos\theta}{4\sqrt{(1-\rho\cos\theta)^3}} - \frac{\kappa J_1(\kappa\rho)}{2\sqrt{1-\rho\cos\theta}} \right] \cdot \left[\cos(m+1)\phi - \cos(m-1)\phi \right] e^{i\omega t} + \frac{m J_0(\kappa\rho)\cos\theta}{2\sqrt{(1-\rho\cos\theta)^3}} \cdot \left[\cos(m+1)\phi + \cos(m-1)\phi \right] e^{i\omega t} \right\} \quad (70)$$

$$B_\phi = -i \frac{\omega\epsilon\mu\kappa J_1(\kappa\rho)\sin\theta}{2\sqrt{1-\rho\cos\theta}} \left[\sin(m+1)\phi + \sin(m-1)\phi \right] e^{i\omega t}. \quad (71)$$

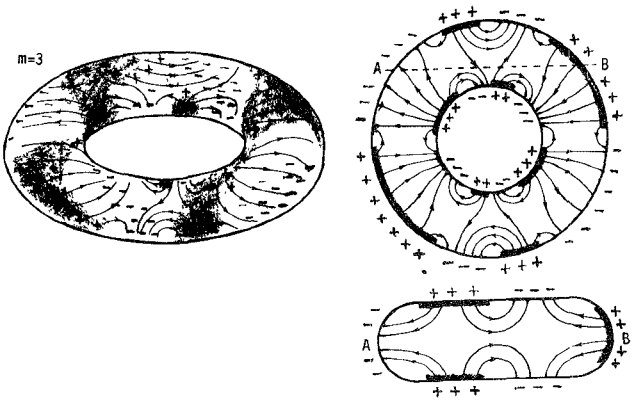

Fig. 12. Toroidal mode of third type. Electric field and surface charge distribution.

For the surface charge density we get

$$\sigma \sim \frac{(1+3\cos^2\theta)\rho_0 - 2\cos\theta}{2\rho_0\sqrt{(1-\rho_0\cos\theta)^3}} \left[\sin(m+1)\phi + \sin(m-1)\phi \right] e^{i\omega t} + \frac{m}{\sqrt{(1-\rho_0\cos\theta)^3}} \left[\sin(m+1)\phi - \sin(m-1)\phi \right] e^{i\omega t}. \quad (72)$$

The charge densities and the electric field lines are represented in Figs. 10–12. The equations for the magnetic field lines are

$$x = (1-\rho\cos\theta)\cos\phi = k_1 \quad (73)$$

and

$$J_0(\kappa\rho)\sin m\phi \sqrt{\cos\phi} = k_2. \quad (74)$$

The magnetic field lines form again vortices in parallel planes which are situated perpendicular to the plane of the torus. The change of the structure of the field vortices is due to the phase difference $\Delta\phi = \pi/2m$ between (61) and (74). There is no longer a $m=0$ mode. As we see from Figs. 6–12, essential differences appear between the structure of the fields of the second and third type. The $m=1$ mode has a simple quadrupole structure. There are also differences in the structure of the magnetic field vortices.

Remark: If we choose instead of $P_x \neq 0$, $P_y = P_z = 0$, the components of the Hertz vector in the form $P_x = P_z = 0$,

$P_y \neq 0$ we get the same type of waves. They will only be rotated by 90° around the z axis.

VI. Conclusions

We succeeded to obtain the explicit form of the components of the electromagnetic field for the lowest θ modes if condition (15) is satisfied. For each eigenfrequency we obtained three types of eigenfunctions with different symmetries. The symmetry properties of the eigenwaves are related with the way to solve our problem. We used Cartesian components of $\vec{P}$ to obtain the possibility to scalarize the vector wave equations. This leads to eigenmodes with the corresponding symmetry (e.g., the magnetic field lines are situated in planes $z = \text{const}$ or $x = \text{const}$). Another method would lead to eigenmodes of another symmetry, but the number of the eigenmodes must be again three for each frequency, the eigenfrequencies must be also described by (32), and the new eigenmodes must be a superposition of the eigenmodes described by us. It is expected that the experimentally realized eigenmodes consist of a superposition of the eigenmodes described here.

The method used in this paper is valid for the lowest m modes satisfying condition (15). There is a formal similarity between the expression of the eigenfunctions (21) and the corresponding solutions for cylindrical resonators, but in the structure of the electromagnetic field, and in the value of the eigenfrequencies some essential differences appear as a consequence of the toroidal geometry.

The toroidality of the system manifests itself in the appearance of the factor $(1-\rho\cos\theta)^{-1/2}$ in the expression for the components of the Hertz vector (9), which has an influence on the structure of the electromagnetic field and on the value of the eigenfrequencies. As a consequence the expression for the Cartesian components of the Hertz vector cannot be separated with respect of ρ and θ, and a further coupling between ρ, θ, and ϕ appears at the construction of the toroidal components (8) of $\vec{P}$. Therefore, the electromagnetic field has a pronounced three-dimensional character. We simplified this character a little by retaining only the first term of the series (16) in the detailed calculations of the field. In this case the more important symmetry characteristics of the toroidal modes became relevant (see Figs. 4–12) but the modes received are essentially different from the well known TE and TM modes of the straight circular waveguides. This is, e.g., evident from the plane structure of the magnetic field and from the ϕ dependence of the field components (see, e.g., (60), (61), (73), and (74)). A superposition of the eigenmodes described by us leads to TE and TM configuration only in very particular cases [9].

A direct consequence of the toroidality is also that in the expression of the eigenfrequency $m^2 - 1/4$ appears instead of m^2.

The limit $\rho \to 0$, $m \to \infty$ coincides with the corresponding limit for the thin straight cylindrical resonators.

The method described can be generalized to other systems with complicated geometries. It was used to describe also the eigenmodes in toroidal systems containing plasma and in coaxial toroidal systems [9] or to solve force-free three-dimensional toroidal MHD equilibria [10].

Acknowledgment

R. Deutsch acknowledges the support of the Österreichischer Fonds zur Förderung der wissenschaftlichen Forschung. Both authors acknowledge the technical support of Mr. Ramberger, who checked some of the calculations, and of Mr. Leubner, who helped with the production of the figures and the plotting process.

References

[1] L. Lewin, Department of Electrical Engineering, University of Boulder, CO, private communication, 1977.
[2] F. Cap and R. Deutsch, "Toroidal electromagnetic modes in isotropic homogeneous plasma and in vacuum," presented at the Third Int. Congress on Waves and Instabilities, in Plasmas, Paris, June 27–July 2, 1977.
[3] M. Brambilla and V. Finzi, "Electromagnetic eigenmodes of the toroidal cavity," *IEEE Trans. Plasma Sci.*, vol. PS-2, pp. 112–114, Sept. 1974.
[4] F. Cap, "Remarks on toroidal problems," *Beiträge zur Plasmaphysik.*
[5] F. Cap, R. Deutsch, D. Floriani, P. Rosenau, and S. Zygelman, "Ahnlichkeitstransformationen in der theoretischen Physik und in der Plasmaphysik," Schlubericht, UNICP-SWD76, Forschungsprojekt 1258, Inst. of Theor. Phys. Univ. Innsbruck, Mar. 1976.
[6] J. Zagrodziński, "Electromagnetic field in rotational coordinates," *J. Phys. A: Math. Gen.*, vol. 10, pp. 823–831, no. 5, 1977.
[7] F. Cap, "The radome problem," Research Report 55-1719, Glenn L. Martin Comp., Baltimore 3, MD., July 1955.
[8] P. Moon and D. E. Spencer, *Field Theory Handbook*. Berlin, Germany: Springer, 1961, 101.
[9] R. Deutsch, "Toroidal electromagnetic modes in a torus containing plasma and in coaxial toroidal systems," *IEEE Trans. Microwave Theory Tech.*, submitted for publication.
[10] F. Cap, "Exact force-free three dimensional toroidal MHD-equilibria and field-reversal," to be published.
[11] R. Deutsch, "Toroidal resonator with a conducting separating wall," *IEEE Trans. Microwave Theory Tech.*, submitted for publication.